

Dear Author,

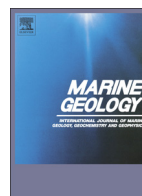
Please, note that changes made to the HTML content will be added to the article before publication, but are not reflected in this PDF.

Note also that this file should not be used for submitting corrections.



Contents lists available at ScienceDirect

## Marine Geology

journal homepage: [www.elsevier.com/locate/margeo](http://www.elsevier.com/locate/margeo)

# Q1 Are large submarine landslides temporally random or do uncertainties in available age constraints make it impossible to tell?

Q2 E. Pope<sup>a,\*</sup>, P.J. Talling<sup>a</sup>, M. Urlaub<sup>b</sup>, J.E. Hunt<sup>a</sup>, M.A. Clare<sup>a</sup>, P. Challenor<sup>c</sup>

<sup>a</sup> National Oceanography Centre, Southampton, European Way, Southampton SO14 3ZH, UK

<sup>b</sup> GEOMAR Helmholtz Centre for Ocean Research Kiel, Wischhofstr. 1–3, 24148 Kiel, Germany

<sup>c</sup> College of Engineering, Mathematics and Physical Sciences, Harrison Building, North Park Road, EX4 4QF, UK

## ARTICLE INFO

## Article history:

Received 15 April 2015

Received in revised form 18 July 2015

Accepted 24 July 2015

Available online xxxx

## Keywords:

Submarine landslides

Sea level

Timing

Tsunami

## ABSTRACT

Large ( $>1 \text{ km}^3$ ) submarine landslides can potentially generate very destructive tsunamis and damage expensive sea floor infrastructure. It is therefore important to understand their frequency and triggers, and whether their frequency is likely to change significantly due to future climatic and sea level change. It is expensive to both collect seafloor samples and to date landslides accurately; therefore we need to know how many landslides we need to date, and with what precision, to answer whether sea level is a statistically significant control. Previous non-statistical analyses have proposed that there is strong correlation between climate driven changes and landslide frequency. In contrast, a recent statistical analysis by Urlaub et al. (2013) of a global compilation of 41 large ( $>1 \text{ km}^3$ ) submarine landslide ages in the last 30 ka concluded that these ages have a temporally random distribution. This would suggest that landslide frequency is not strongly controlled by a single non-random global factor, such as eustatic sea level. However, there are considerable uncertainties surrounding the age of almost all large landslides, as noted by Urlaub et al. (2013). This contribution answers a key question that Urlaub et al. (2013) posed, but could not address – are large submarine landslides in this global record indeed temporally random, or are the uncertainties in landslide ages simply too great to tell? We use simulated age distributions in order to determine the significance of available age constraints from real submarine landslides. First, it is shown that realistic average uncertainties in landslide ages of  $\pm 3 \text{ kyr}$  may indeed result in a near-random distribution of ages, even where there are non-random triggers such as sea level. Second, we show how combination of non-random landslide ages from just 3 different settings, can easily produce an apparently random distribution if the landslides from different settings are out of phase. Third, if landslide frequency was directly proportional to sea level, we show that at least 10 to 53 landslides would need to be dated perfectly globally – to show this correlation. We conclude that it is prudent to focus on well-dated landslides from one setting with similar triggers, rather than having a poorly calibrated understanding of ages in multiple settings.

© 2015 Published by Elsevier B.V.

## 1. Introduction

Submarine landslides are one of the volumetrically most important mechanisms through which sediment is transported from the continental slope to the deep ocean (Hühnerbach and Masson, 2004; Masson et al., 2006; Korup, 2012; Talling et al., 2012; Urlaub et al., 2013, 2014). Landslide deposits have been mapped on many continental slopes as disparate as southeast Australia (Clarke et al., 2012) and the Grand Banks, Newfoundland (Piper et al., 1999). Submarine landslides can be far larger than any terrestrial landslide, and can involve the movement of hundreds or even several thousands of cubic kilometres of material (Hampton et al., 1996; Hühnerbach and Masson, 2004; Talling et al., 2007). Perhaps the most remarkable aspect of large submarine landslides is that they typically can occur on very low gradients

of just  $1\text{--}2^\circ$  (Hühnerbach and Masson, 2004; Talling et al., 2007; Urlaub et al., 2012, 2014). Such low gradients are almost always stable on land. Once in motion, the submarine slide mass can entrain ambient seawater and disaggregate to form longer runout sediment flows, known as turbidity currents. These turbidity currents can themselves travel many hundreds of kilometres (Weaver and Kuijpers, 1983), and reach speeds of up to  $\sim 20 \text{ m/s}$  (Piper et al., 1999; Hsu et al., 2008).

Submarine landslides, debris flows and associated turbidity currents may represent significant geohazards. Submarine landslides have the potential to generate damaging tsunamis (Ruffman, 2001; Tappin et al., 2001; Haflidason et al., 2005; Boe et al., 2007; Hornbach et al., 2007); whilst both landslides and turbidity currents can damage expensive sea floor infrastructure, such as that associated with the hydrocarbon industry or seafloor telecommunications (Bruschi et al., 2006; Carter et al., 2009; Parker et al., 2009, 2012). Some authors have argued that the occurrence of large submarine landslides can have significant climatic impacts through the release of large amounts of methane into

\* Corresponding author.

E-mail address: [ed\\_pope@hotmail.co.uk](mailto:ed_pope@hotmail.co.uk) (E. Pope).

the water column and the atmosphere (Kennett et al., 2000; Maslin et al., 2004; Pecher et al., 2005; Vanneste et al., 2006; Beget and Addison, 2007; Paull et al., 2007). Understanding the frequency and triggers of large submarine landslides is therefore important.

### 1.1. Triggering and preconditioning of submarine landslides

A large number of triggers and preconditioning factors have been hypothesised as possible causes for large submarine landslides. Potential preconditioning factors and triggers include earthquakes, rapid sedimentation that leads to high excess pore pressure and conditions close to failure, and gas hydrate dissociation that reduces sediment strength (Hampton et al., 1996; Maslin et al., 1998; Stigall and Dugan, 2010; Goldfinger, 2011; Masson et al., 2011; Talling et al., 2014). However, not all large ( $>7 M_w$ ) earthquakes appear to generate major slides (Völker et al., 2011; Sumner et al., 2013), large submarine landslides occur in locations with slow sediment accumulation (Urlaub et al., 2012), and some landslide headwalls occur in water depths that are too deep for gas hydrate dissociation (Hühnerbach and Masson, 2004). In general, many of these hypotheses for landslide preconditioning and triggering are weakly tested, in part because we are yet to directly monitor large slides in action in sufficient detail (Talling et al., 2014).

### 1.2. Submarine landslide frequency and sea level – previous work

A series of previous studies explored the potential relationship between landslide frequency and sea level. The first set of studies used compilations of landslide ages, typically from widespread locations.

#### 1.2.1. Global databases of landslide ages

The initial analyses did not include full uncertainties in landslide ages, or test the certainty of their conclusions through quantitative statistical methods. These studies suggest that increased landslide frequency occurred during specific periods in glacial cycles, corresponding to sea level low-stands, high-stands, or rapid rates of sea level change. Brothers et al. (2013) identify a causal relationship between sea level rise and landslide triggering. Paull et al. (1996) identify increased numbers of landslides during low-stands related to reduced overburden pressure of the water column on gas hydrate bearing sediments. Leynaud et al. (2009), Maslin et al. (1998, 2004), Lee (2009) and Lebreiro et al. (2009) recognised that different margins responded differently to sea level. For example, low latitude margins experienced more large submarine landslides during low-stands while high latitudes were more likely to see slope failures during rising sea levels or high-stands.

Subsequent analysis has sought to evaluate these qualitative conclusions using statistical approaches. Urlaub et al. (2013) considered a collection of 68 large ( $>1 \text{ km}^3$ ) submarine landslide ages from locations worldwide, which includes the last 120 ka (Fig. 1). This is the largest number of landslide ages yet compiled. It included dates from landslide deposits themselves from open slope failures (but not volcanic island failures) where ages were obtained by radiocarbon AMS measurements or by applying a combination of several methods (e.g. biostratigraphy and oxygen isotopes). It also included large ( $>1 \text{ km}^3$ ) turbidites inferred to be landslide-triggered. Such large volume turbidites are unlikely to be triggered by processes other than slope failure, as their volume far exceeds even the largest historical river flood (Talling et al., 2014). In general, such turbidites will tend to record faster moving landslides that disintegrate to produce turbidity currents. See Urlaub et al. (2013) for a fuller discussion on the consistent selection criteria.

The Urlaub et al. (2013) study took a subset of 41 events in the last 30 ka to analyse statistically from the compiled global database. This subset was chosen to avoid a strong bias due to undersampling of older events, caused by limits to core penetration below the sea floor; most sediment cores extended back to 30 ka, but few reached 120 ka.

The analysis by Urlaub et al. (2013) included the often considerable uncertainties in landslide ages in this analysis (Fig. 1), unlike most previous studies that considered only the calibrated mean ages or most probable ages (Ramsey, 1998). The greatest uncertainties in landslide age typically result from where samples are taken for dating, above and below the landslide or turbidite deposit, rather than the error bars in the (typically AMS radiocarbon) dates themselves. This is discussed more fully in Urlaub et al. (2013), and illustrated by our Fig. 2.

Urlaub et al. (2013) analysed these 41 landslide ages. They first divided their 30 ka study period into a series of equal time intervals, termed bins (e.g. 0–5 kyr, 5–10 kyr, and 10–15 kyr). They then counted the number of landslide ages that fell within each bin. This allowed them to plot the number of bins with a single landslide age, two landslide ages, three landslide ages, and so forth (Urlaub et al., 2013; their Fig. 8a, b). A random number generator was then used to produce a set of synthetic landslide ages, assuming landslide occurrence was temporally random. The same procedure was followed to count the number of synthetic landslide ages in each bin, and the number of bins with one, two or more landslide ages. It was found that there was no statistically significant difference between the frequency of bins with 1, 2, 3 or more landslide ages, both real and synthetic landslide ages using the  $\chi^2$  statistic (their Fig. 8c). The duration of bins was varied between 1 kyr and 5 kyr, as this affects the frequency distribution of the landslide ages. Both the ‘best guess’ landslide ages, and landslide ages acknowledging age uncertainty were tested in this way. In each case, landslide ages were described by the  $\chi^2$  statistic as occurring randomly, such that they approximated a Poisson distribution (Urlaub et al., 2013).

#### 1.2.2. Landslide recurrence intervals on the margins of a single basin

A second type of study used different types of data and statistical methods to consider the recurrence intervals of landslides around the margins of a single sedimentary basin (Hunt et al., 2013; Clare et al., 2014), as opposed to a global dataset of landslide ages. These studies used large volume turbidites as a proxy for large landslides that disintegrate, which are presumably faster moving. Clare et al. (2014) considered large ( $>0.1 \text{ km}^3$  in these cases) landslide turbidite recurrence intervals in three disparate abyssal plain sequences of variable age, whilst Hunt et al. (2013) considered landslide–turbidites in the Agadir Basin offshore NW Africa. They compared the frequency distribution of landslide turbidite recurrence intervals, with a Poisson frequency distribution. It was found that the frequency distribution of the landslide–turbidite recurrence intervals did not differ significantly from the (Poisson) distribution produced by a temporally random process. Both of these studies therefore suggest that large landslides, which disintegrate to form long run-out turbidity currents, are temporally random, or near random (Hunt et al., 2013; Clare et al., 2014).

#### 1.2.3. Discrete vs continuous data

The Urlaub et al. (2013), Hunt et al. (2013) and Clare et al. (2014) studies all concluded that the occurrence of submarine landslides followed a Poisson distribution. A Poisson distribution implies a lack of memory in the system which it is describing, such that the probability of a new event occurring is independent of the time since the last. The methodology used by the different studies is dependent on the type of data. The global nature of the Urlaub et al. (2013) study and the uncertainty regarding the duration of inter-event timing required the study to use ‘discrete’ (count) data that was binned. The number of landslides within a given time period was compared to the number that would theoretically be produced by a random process. In contrast, the availability of landslide–turbidite recurrence intervals (inter-event time) allowed Hunt et al. (2013) and Clare et al. (2014) to use ‘continuous’ data. This study follows the approach of Urlaub et al. (2013) and therefore uses discrete data.

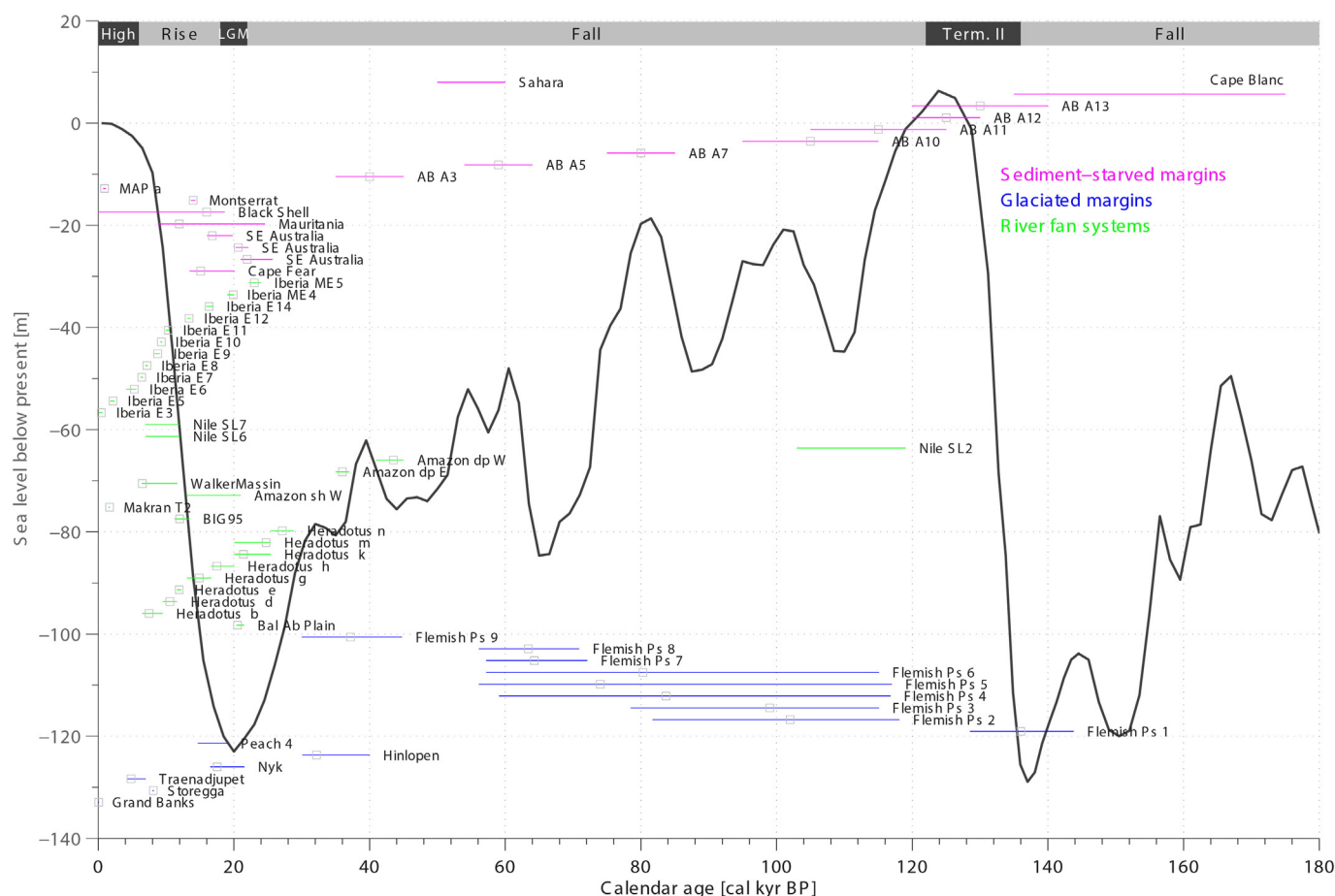


**Fig. 1.** Global mean sea level (black curve, [Waelbroeck et al., 2002](#)) plotted with submarine landslide ages, which includes their uncertainty intervals (from [Urlaub et al., 2013](#)). If available, the age with the highest probability is shown by a grey square. The colour of the uncertainty line indicates the sedimentary environment. The grey time line on the upper part of the figure indicates the sea level pattern. (For interpretation of the references to colour in this figure legend, the reader is referred to the web version of this article.)

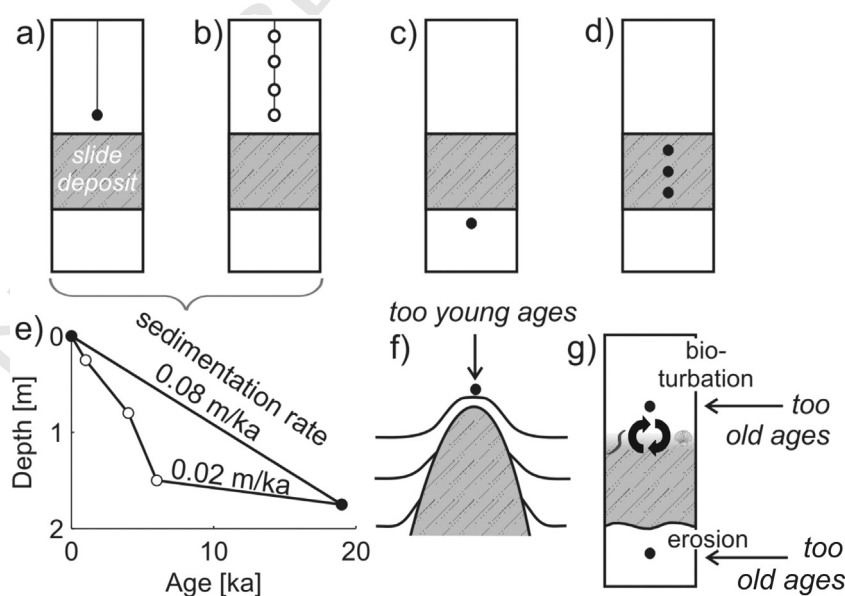


**Fig. 2.** Different sampling strategies for radiocarbon dating of submarine landslides. The rectangles represent sediment cores with hemipelagic background sedimentation (white) and a landslide deposit (grey). Open and filled black circles indicate the position of the sample. A minimum age is obtained by taking one (a) or several samples (b) from the hemipelagic unit above the landslide deposit. A maximum age is obtained when samples are either taken from the hemipelagic unit below (c) or within (d) the failure deposit. A linear average sedimentation rate for the core based on one sample can be significantly different from actual temporary sedimentation rates (e), which can be calculated when several samples between the top of the core and the top of the failure deposit are available. Samples above the deposit can give an age too young if located on a local high (f) and bioturbation on the top as well as erosion at the base of the failed deposit (g) are possible sources of uncertainty to the estimated ages.

Fig. 1 from [Urlaub et al., 2013](#).



### 1.3. Rationale for this study – why is it necessary, novel and valuable?

This study answers the key outstanding questions that remain from the study of [Urlaub et al. \(2013\)](#), which concluded that large landslide ages were temporally random. They posed, but failed to answer the important question: *is this because large submarine landslide ages are temporally random, or is it because the uncertainties in the ages are too large to tell?* Here we provide a novel answer to that question. It is important to understand what this compilation of ages is telling us about landslide frequency, as each landslide age has been costly to acquire. For example, if landslide ages actually correlate perfectly with global sea level, is it likely that uncertainties in measuring their ages could easily produce an apparently random age distribution?

We also address two further key questions that have not previously been addressed. First, *how easy is it to produce temporally random landslide ages simply from combining (non-random) landslide ages from multiple settings with different triggers and preconditioning factors?* It is important to answer this question because this is indeed the situation for most global datasets of landslide ages, which combine dates from different settings, including that presented by [Urlaub et al. \(2013\)](#). Second, *how many submarine landslides do we need to date, and with what precision, in order to test whether landslide frequency is controlled strongly by global sea level?* This is important because it is costly to sample and date submarine landslides. We need to know what the most effective future strategy will be for determining whether landslides and sea level are linked.

#### 1.3.1. Why use simulated landslide ages?

Our aim is to understand the significance of the available dates, with their uncertainties, from real large submarine landslides (such as compiled by [Urlaub et al., 2013](#)). However, to answer the three key science questions outlined above we first consider series of simulated landslide ages. We do not consider landslide ages from the original [Urlaub et al., 2013](#) database. Our approach allows us to determine whether simulated landslide ages, which are perfectly known and lack any uncertainties, can form temporally random patterns once reasonable age uncertainties are added. Such an approach cannot be taken with real landslide ages, whose ages all have significant uncertainties. Similarly, the simulated ages allow us to investigate the ease with which perfectly known landslide ages from different settings (with variable triggers and preconditioning factors) can be combined to form apparently temporally random landslide ages. Finally, these simulated landslide ages allow us to test how many landslide ages are needed to identify a strong sea level control. It is impossible to do this using real landslide ages that all have different error bars, and for which we do not know there is a perfect association with sea level. So these synthetic landslide ages allow us to fix key parameters (e.g. error bars), to answer key questions about the real field datasets. An additional advantage of such simulated ages is that potential biases are avoided, such as the ages mostly coming from the northeast Atlantic as is the case for [Urlaub et al. \(2013\)](#).

## 2. Methods

This section first outlines the statistical method used to test for randomness in landslide ages ([Section 2.1](#)). It then describes how simulated (artificial) catalogues of landslide ages were created that are non-random, and have perfectly known ages ([Section 2.2](#)). [Sections 2.2.1 and 2.2.2](#) outline how realistic uncertainties (error bars) were added to these simulated ages and how changes to the 1 kyr bins were investigated with regard to how event frequency is measured. [Section 2.3](#) describes how simulated landslide ages from multiple settings are combined. Finally, [Section 2.4](#) outlines the methodology used to test how many landslides are needed to identify a strong sea level control whose rationale for choosing rather than other variables is detailed in [Section 2.5](#).

### 2.1. $\chi^2$ test for a temporally random (Poisson) distribution

To test for a temporally random distribution, we use the  $\chi^2$  methodology outlined by [Urlaub et al. \(2013\)](#). The  $\chi^2$  test assesses the goodness of fit of a dataset to a temporally random distribution by analysing whether there are statistically significant peaks, clusters or trends within the dataset ([Swan and Sandilands, 1995](#)). As the  $\chi^2$  test is testing a temporal process, the data are split into time intervals of certain lengths known as bins. The number of bins containing a certain number of landslides is counted. These are then compared to the number of bins with an expected number of events according to a Poisson model generated from the same number of events and bins. The distribution of events is considered random if the  $\chi^2$  value is smaller than the  $\chi^2$  critical value. The  $\chi^2$  critical value is obtained from a look-up table depending on the number of classes observed (see [Swan and Sandilands \(1995\)](#) for further details). The critical values at the 95% confidence level can be seen in [Table 1](#).

In addition to the  $\chi^2$  test set out in ([Urlaub et al., 2013](#)) we also use the likelihood ratio  $\chi^2$  test ([Kendall et al., 1999](#)). The likelihood ratio  $\chi^2$  test is defined as:

$$G^2 = 2 \sum \left[ O_j \log \frac{O_j}{E_j} \right] \quad (1)$$

where  $O_j$  is the number of bins observed with a given number of events and  $E_j$  is the number of bins expected with a given number of events ([Kendall et al., 1999](#)). The likelihood ratio test provides a means to analyse the likelihood of the landslide ages being random or non-random. If the likelihood ratio exceeds a critical value then we have reason to reject the distribution prescribed by the  $\chi^2$  statistic. The critical value is obtained from the  $\chi^2$  look-up table according to the number of classes observed. Using the likelihood ratio in addition to the  $\chi^2$  statistic provides a more rigorous analysis.

### 2.2. Creating simulated non-random landslides with perfectly known ages

This study initially uses a set of artificially generated landslide ages that are known perfectly, without any uncertainty, for reasons set out in [Section 1.3.1](#). Four types of non-random landslide age patterns were investigated. Our aim was to understand how many of these perfectly known landslide ages we would need to measure to show if they are random or non-random. [Fig. 3](#) provides a visual explanation of each

**Table 1**  
 $\chi^2$  critical values at the 95% confidence interval. A critical value is selected according to the number of classes being compared, i.e. if three classes are being compared such that there are bins with 0, 1, and 2 landslides then the critical value for 2 degrees of freedom ( $\nu$ ) will be selected. If there are four classes being compared such that there are bins with 0, 1, 2, and 3 landslides then the critical value for 3  $\nu$  will be chosen and so on. When the calculated  $\chi^2$  value exceeds the appropriate critical value the distribution of events is deemed non-random.

$\nu$	95%	
1	3.841	t1.15
2	5.991	t1.16
3	7.815	t1.17
4	9.488	t1.18
5	11.07	t1.19
6	12.592	t1.20
7	14.067	t1.21
8	15.507	t1.22
9	16.919	t1.23
10	18.307	t1.24

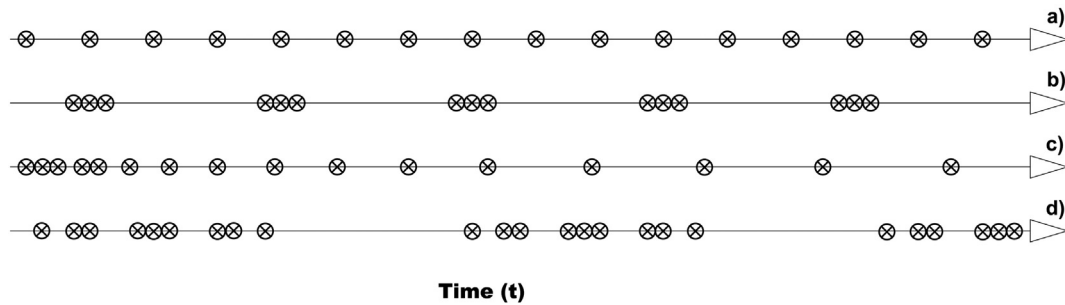


**Fig. 3.** Plot showing examples of the ordered distributions used to analyse the impact of age uncertainties. Landslides with a) perfectly periodic patterns, b) clustered patterns, c) increasing inter-event time patterns, d) patterned patterns.  
Swan and Sandilands, 1995.

type of non-random age distribution. These four types of landslides ages are perfectly periodic, clustered, with linearly increasing inter-event times, or patterned in time (Fig. 3; Swan and Sandilands, 1995). Examples of functions used to generate perfectly periodic (Eq. (3)), clustered (Eq. (4)) and linearly increasing inter-event times (Eq. (5)) are shown below. Events are considered to occur when the value of  $f(x)$  is equal to 1.

$$f(x) = \sin(x) \quad (3)$$

$$f(x) = \sin(x) + \frac{1}{2} \sin x + 0.1 \quad (4)$$

$$f(x) = \sin(x^x) \quad (5)$$

Patterned landslide ages were produced by using more than one of these generating functions. These patterned events were manipulated to change their average event frequency (Fig. 3). The number of events within an individual simulated catalogue of landslide ages ranged from 5 to 100. This range was chosen because 5 is the minimum number of events required for the  $\chi^2$  test, and 100 events is about 2.5 times more events than in the Urlaub et al. (2013) global compilation. It thus captures a reasonable minimum and maximum value for the number of available landslide ages. These patterns were used to examine if we could identify whether the occurrence of landslides in these simulated records was indeed non-random.

#### 2.2.1. Addition of uncertainties in ages

Age uncertainties were subsequently applied to the patterns of landslides outlined in Section 2.2 in a number of different ways. First, age uncertainties of up to  $\pm 0.75$  kyr were applied uniformly to all landslide ages. This was done because  $\pm 0.75$  kyr represented an age uncertainty large enough for any event to be moved by at least one bin (each bin is 1 kyr). The choice of limiting uniform error results from the  $\chi^2$  test assessing the distribution through the use of bins. The use of bins combined with uniform age uncertainty means that the  $\chi^2$  test is not sensitive to the temporal order of events. Thus, with uniform age uncertainty of  $\pm 0.75$  kyr, events are able to reverse their temporal order, although the  $\chi^2$  test will not recognise this.

Second, age uncertainties of a random duration between 0 kyr and 3 kyr were applied to events. Both the size of age uncertainty and the event to which it was applied were selected using random number generators. Our choice of a range between 0 and 3 kyr was informed by the uncertainties in age of river fan systems in the Urlaub et al. (2013) study, which have a mean error of 2.34 kyr (Rothwell et al., 1998; Reeder et al., 2000, 2002; Lastras et al., 2004; Maslin et al., 2005; Garziglia et al., 2008; Gracia et al., 2010; Bourget et al., 2011; Masson et al., 2011, 2013). This is the smallest mean uncertainty for any of the settings considered by Urlaub et al. (2013).

Third, ever increasing age uncertainties were applied to events. Age uncertainties increased progressively in accordance with the age of the event that it was being applied to, i.e. the youngest event did not have an age uncertainty whilst the age uncertainty of the oldest event was the largest (see Fig. 4). The largest age uncertainty applied was 20 kyr ( $\pm 10$  kyr) reflecting the global record used by the Urlaub et al. (2013) study as the greatest age uncertainty present in this record was 19.98 kyr ( $\pm 9.99$  kyr) (Reeder et al., 2002).

#### 2.2.2. Moving the positions of the 1 kyr bins

Landslide ages were assigned to 1 kyr duration bins (0–1 ka, 1–2 ka, 2–3 ka, etc.) in order to produce a histogram of landslide frequency. Urlaub et al. (2013) noted that the position and duration of these bins could affect the analysis. We chose bin durations of 1 kyr for the following reason; that linking landslide frequency to changing environmental factors, such as sea level variations, necessitates that the bin size is sufficiently small to capture the environmental change under consideration. In the case of sea level change, 1 kyr bin size is reasonably appropriate (Waelbroeck et al., 2002). The position of the 1 kyr bins was varied during the analysis outlined in Sections 2.2 and 2.2.1 to test the extent to which bin position affects our ability to recognise whether landslides are non-random.

#### 2.3. Landslides from multiple settings

We also simulate different landslides coming from multiple settings. Each setting was defined to have a perfectly periodic (non-random) sequence (Fig. 3a), but with a different return period. For example, one setting was given a uniform recurrence interval of 1.5 kyr, another 2 kyr, and the third 3.5 kyr. Landslide ages from these multiple settings were then combined into one overall catalogue and tested for a temporally random sequence as a single dataset. This was done to simulate the generation of a global record of landslides combining different margin types, including glaciated, fluvial and sediment starved, as was seen in Urlaub et al. (2013) or different geographical margins around one basin (Clare et al., 2014) (Fig. 5). The datasets were then manipulated individually and as a single catalogue, by introducing different size error bars to the landslide ages and changing the position of the 1 kyr bins. This methodology was then carried out for the other pattern types seen in Fig. 3. It is important to test the role of multiple settings as global datasets of events will include landslides from multiple different margin types, whilst basin records will include turbidites derived from landslides which may have different environmental settings.

#### 2.4. Simulated landslide ages whose frequency is dependent on sea level

A third series of landslide ages were generated to analyse the number of events needed to establish with reasonable certainty that global landslide frequency is controlled strongly by sea level. The frequency of the landslides in this catalogue was defined to be directly proportional to

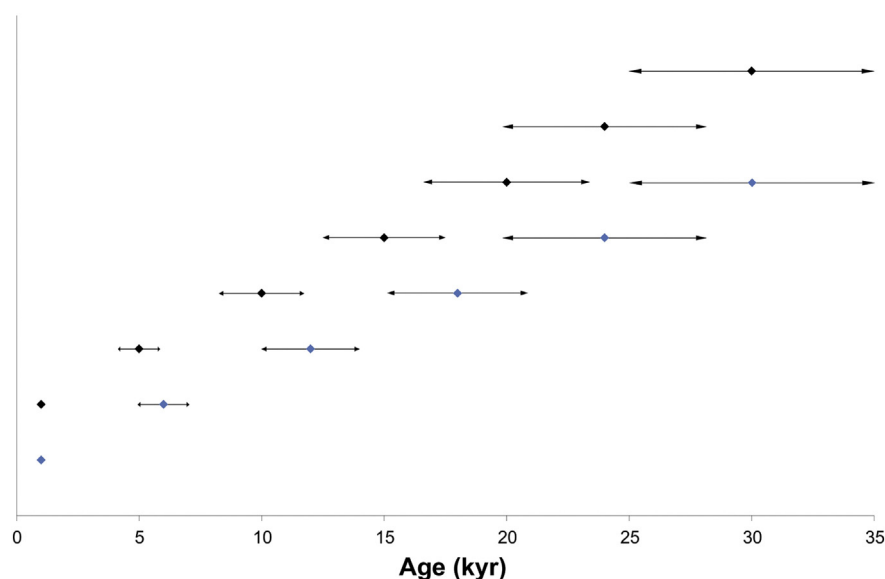


**Fig. 4.** Plot showing a schematic of the application of ever increasing age uncertainties. Black and blue diamonds represent two different patterns of landslides. Black arrows represent age uncertainties which increase as the landslide gets older within each pattern.

sea level, using a global eustatic sea level curve for the last 30 ka (Waelbroeck et al., 2002). Event frequency was simulated to be highest during the last 1 ka in accordance with the highest sea level, whilst the lowest frequency occurred around the last glacial maximum ~20 ka. A directly proportional relationship was chosen in order for there to be the strongest possible relationship between sea level and event frequency; thus it serves to enable us to identify the fewest number of events needed as part of a best case scenario to link the two processes. It also acts as a starting point for linking other processes to landslide occurrence.

This artificial catalogue of landslide ages contained 67 entries, which were numbered from 0 to 66. We then explored how many events were needed to identify sea level control. Beginning with one event from the catalogue, events were added randomly to our analysis until all 67 were included. This mimics the discovery and dating of submarine landslides through continued field investigations. Bins with durations of 1 kyr are used to order to replicate the precision needed to link event frequency to sea level. The catalogue was chosen to contain 67 events as this is greater than the current global catalogue of well dated landslides for the last 30 ka (i.e. 41 events; Urlaub et al., 2013), whilst being within

the same order of magnitude thus acting as a useful comparison to the global landslide record.

#### 2.5. Why choose to investigate landslide frequency proportional to sea level?

We specifically investigate sea level due to its link to current anthropogenic climate change and concerns regarding the consequence of future sea level rise on landslide frequency (Maslin et al., 2004, 2005; Owen et al., 2007; Lee, 2009). Using the global sea level curve for the last 30 ka provides us with the simplest test of how many landslide events we would need to date to identify a non-random temporal distribution of events. This 30 kyr time period, used in the Urlaub et al. (2013) study, represents just over half a glacial cycle. Sea level begins the period during a low stand and rises to the end of the period. When the relationship between sea level and landslide frequency is linearly proportional over the last 30 ka, the distribution of landslide ages is a close approximation to a trend distribution (Fig. 3c). If the  $\chi^2$  test is unable to identify this relationship we are unlikely to be able to identify a relationship between another variable and landslide frequency.

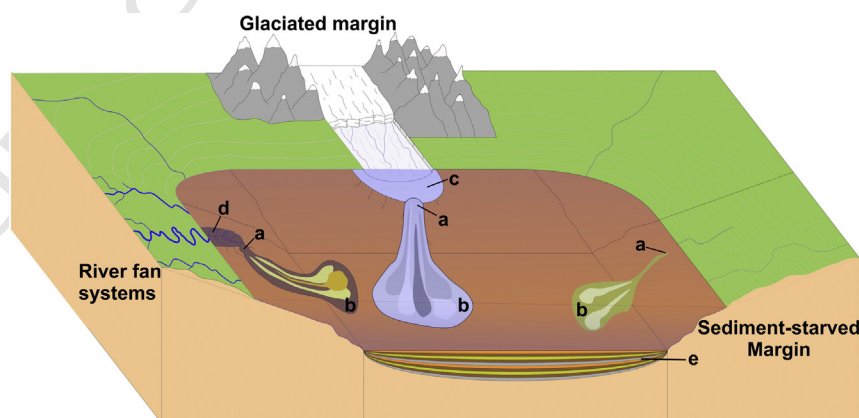


**Fig. 5.** Three separate sedimentary systems feeding into one ocean basin. Each system is likely to have different characteristic landslide recurrence intervals due to different local environmental factors. River fan systems experience the highest sediment input during deglaciation or lowstands, depending on latitude, as rivers efficiently transport terrestrial sediment (Covault and Graham, 2010; Urlaub et al., 2013). Glaciated margins are strongly influenced by climatic cycles due to the direct influence of growing and shrinking ice sheets and the position of ice streams (Lee, 2009) in terms of both local sea level and the location and timing of sediment delivery (Dowdeswell et al., 1996). Sediment starved margins are characterised by lower sediment deposition rates as they have not been affected by glaciation and are located away from major river fan systems. Labels (a) landslide headscarp, (b) landslide deposits, (c) trough mouth fan, (d) river fan delta, (e) interbedded sequence of background hemipelagic and sediment density flow deposits.



Importantly, whilst we analyse sea level, this analysis is also able to represent a proportionally linear response of landslide frequency to rate of sea level change over the same period. In a catalogue of 67 landslides where landslide frequency was linearly proportional to rate of sea level change, the frequency distribution using 1 kyr bins would be the same as the sea level controlled example. The only difference between the catalogues would be that they are temporally offset from each other. Crucially, the  $\chi^2$  methodology outlined using bins does not recognise the temporal order of events (see Section 2.2.1.) merely the frequency of events in different bins. The  $\chi^2$  test used would therefore not recognise any difference between a landslide dataset linearly proportional to sea level and a landslide dataset linearly proportional to sea level change if half or a full sea level cycle is included within the period of study.

### 3. Results

We now address the three main questions that form the aims of this study.

#### 3.1. Are large landslides temporally random, or are age uncertainties too large to tell?

##### 3.1.1. How many perfectly known landslide ages are necessary to show they are non-random?

Simulated landslide ages were generated for the last 30 ka that were perfectly non-random and whose ages were known perfectly. It was found that when there were over 40 dated landslides in the distribution, we could always correctly determine that landslide occurrence was non-random. Where samples of >40 ages were taken from the distribution types, the  $\chi^2$  statistic allowed us to reject the hypothesis of temporal randomness for all the pattern types.

When samples of <40 ages were analysed, the results were more variable. Table 2 contains the results for the iteration of each landslide dataset pattern containing the largest number of events that appeared temporally random according to the  $\chi^2$  statistic. Each of these patterns is also displayed in Fig. 6. Here, we show how the  $\chi^2$  statistic varies as the number of landslides in each pattern changes. The apparent cyclical nature of the  $\chi^2$  statistic value is a consequence of the methodology using discrete data and the relative numbers of bins with events in them. For example, in Fig. 6a the  $\chi^2$  statistic is sensitive to the relative numbers of events in each bin, i.e. how many bins contain 2 landslides and how many contain 3. The  $\chi^2$  statistic therefore peaks when all of the bins have the same number of events in before declining until 50% of the bins contain one number of landslides while the other 50% contain a different number of landslides. The  $\chi^2$  statistic subsequently rises as the percentage of bins with the same number within them increases.

Perfectly periodic distributions were only considered random when the event dataset contained 14 events or fewer (Fig. 6a). At 14 ages the event dataset returned a critical value of 3.814 which was below the critical  $\chi^2$  value of 3.841 at the 95% confidence interval. The likelihood ratio statistic supports identification of this distribution as random; 0.663 is well below the critical value of 3.841. Non-random landslide datasets with linearly increasing inter-event times were considered random when they contained 17 ages or fewer (Fig. 6c). Considering 17 ages the dataset returned a critical value of 3.212 which was below the critical  $\chi^2$  value of 3.841 at the 95% confidence interval. The

likelihood ratio (0.553 does not exceed the critical value of 3.841), which supports this evaluation.

The relationship between number of events and the ability of the  $\chi^2$  statistic to recognise non-random recurrence of events was found to be more complicated for clustered and patterned datasets and showed an important influence of bin position. For clustered landslide patterns, the  $\chi^2$  statistic considered datasets with 14 events or fewer to be temporally random. For a dataset containing 14 ages, the  $\chi^2$  critical value was 3.525 which was below the critical value of 3.841 required to show non-randomness. The maximum number of ages as part of a clustered dataset of landslide ages which was considered random was 37 (Fig. 6b). The  $\chi^2$  statistic returned for the clustered dataset containing 37 ages was 2.798 compared to the critical value of 3.841. The likelihood ratio supports this interpretation although its value (3.423) is almost at parity with the critical value (3.841). This suggests that small changes could alter the interpretation of the distribution which supports the range of distributions interpreted for patterns containing between 14 and 37 ages. Datasets containing between 14 and 37 ages were also often considered random. However, movement of the 1 kyr bins resulted in many of these datasets being shown to be temporally non-random.

The range of patterned (Fig. 3d) landslide age datasets considered temporally random exceeded that demonstrated by the clustered datasets. No patterned dataset with 14 ages or fewer could be discerned from a random distribution. However, a dataset with 39 patterned ages could not be accepted as different to a random distribution according to the  $\chi^2$  statistic (Fig. 6d). It had a  $\chi^2$  critical value of 4.94 which was less than the 5.991 critical value required to be considered non-random at the 95% confidence interval (the likelihood ratio value was 2.829 compared to a critical value of 5.991). The  $\chi^2$  statistic considered different patterned landslide age datasets containing between 14 and 39 events, which were both temporally random and non-random. For many datasets the position of the bins was crucial. It was found that movement of the bins often altered whether the dataset was considered temporally random at the 95% confidence interval.

##### 3.1.2. Introduction of more realistic uncertainties (error bars) in landslide ages

We first introduced uniform age uncertainties of up to  $\pm 0.5$  kyr to the four different non-random landslide age patterns. In each case we considered more than 40 landslide events. This did not produce any submarine landslide age distributions that appeared temporally random according to the  $\chi^2$  statistic. Similarly, the introduction of error bars in landslide ages between  $\pm 0.25$  kyr and  $\pm 0.75$  kyr produced, with the exception of a number of patterned landslide age datasets, no distributions which appeared temporally random with >40 landslides.

In some cases it was found that movement of the bins resulted in the patterned landslide age datasets appearing to be non-random, which had previously been determined as random. For example, movement of the 1 kyr bins resulted in the same dataset, with 55 ages, having  $\chi^2$  values of between 12.121 and 7.533 with the  $\chi^2$  critical value being 9.488 (the likelihood-ratio test for these examples being 4.535 and 3.427 respectively). This implies that as age uncertainties increase the  $\chi^2$  test becomes increasingly sensitive to bin position due to its inability to recognise temporal order.

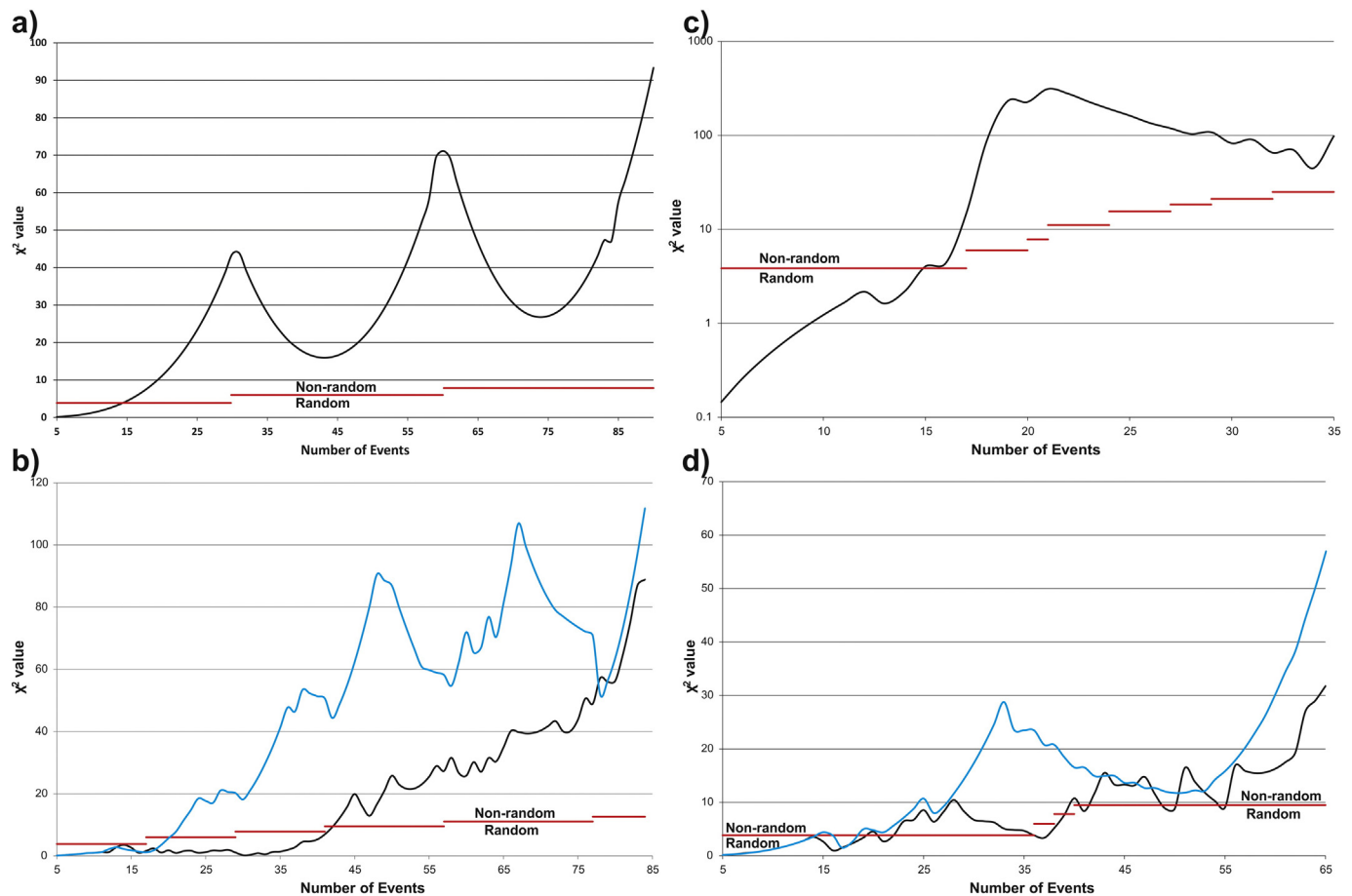
The impact of age uncertainties of  $\pm 0.75$  kyr on landslide patterns is shown in Fig. 7. Here, we show the impact of  $\pm 0.75$  kyr on the  $\chi^2$  value to the landslide patterns shown in Fig. 6. Fig. 7a–d all show that age

Table 2

$\chi^2$  and likelihood ratio results for landslide age patterns containing the greatest number of events with no age uncertainties which appear to be random according to the  $\chi^2$  test.

Perfectly periodic	14	16 (17.60)	14 (9.39)	0 (2.50)	0 (0.444)	3.841	2.9063	0.663
Clustered	37	10 (8.74)	8 (10.78)	7 (6.65)	5 (12.73)	3.841	2.7982	3.423
Linearly increasing inter-event times	17	15 (17.02)	14 (9.65)	0 (2.73)	1 (0.516)	3.841	3.212	3.744
Patterned	39	6 (8.16)	15 (10.63)	5 (6.91)	4 (2.99)	5.991	4.94	2.829





**Fig. 6.** Plot showing how the  $\chi^2$  statistic value changes with increasing numbers of events in each pattern type when ages are perfectly known. a) The impact of increasing numbers of landslides on the  $\chi^2$  statistic where the pattern is perfectly periodic. b) The impact of increasing numbers of landslides on the  $\chi^2$  statistic where the pattern is clustered. The black line represents the pattern which contained the largest number of landslides before the  $\chi^2$  statistic recognised it as non-random. The blue line represents the pattern which contained the smallest number of landslides before the  $\chi^2$  statistic recognised it as non-random. c) The impact of increasing numbers of landslides on the  $\chi^2$  statistic where the pattern has increasing inter-event times. d) The impact of increasing numbers of landslides on the  $\chi^2$  statistic where the pattern is patterned. The black line represents the pattern which contained the largest number of landslides before the  $\chi^2$  statistic recognised it as non-random. The blue line represents the pattern which contained the smallest number of landslides before the  $\chi^2$  statistic recognised it as non-random. In a–d the red line represents the  $\chi^2$  critical value; one the  $\chi^2$  statistic is above the critical value the pattern of landslides is no longer considered random. (For interpretation of the references to colour in this figure legend, the reader is referred to the web version of this article.)

uncertainty can reduce the  $\chi^2$  statistic value of non-random patterns. However, Fig. 7a, b and d all show that where patterns of landslides contain relatively few events, the response to the age uncertainty can be for the pattern to increase the  $\chi^2$  statistic value and thus appear much less random than when the pattern had no age uncertainty associated with it. Fig. 7c implies that where patterns of landslides have linearly increasing inter-event times the impact of introducing age uncertainties is primarily to reduce the  $\chi^2$  statistic value.

Further analysis of larger error bars in landslide ages involved two approaches. First, randomly generated age uncertainties of between 0 kyr and 3 kyr were assigned to events randomly using a random number generator. This allowed us to define the threshold number of landslide events, which have a certain age uncertainty, that are needed to make non-random landslides appear temporally random. This threshold number of landslides with age uncertainties varied depending on the original pattern (periodic, clustered, etc.) and the number of events within the pattern. Second, it was assumed that age uncertainties increased linearly for progressively older landslides up to 20 kyr. This approach resulted in almost all of the datasets we considered, appearing temporally random. The apparent randomness was caused predominantly by the larger age uncertainties (up to 20 kyr) on the older landslides in each distribution.

Urlaub et al. (2013) considered 41 landslide ages in the last 30 kyr from a series of different settings. The 24 examples from river fed

systems have the smallest average error bars (2.34 kyr). Their landslide ages from other settings have even larger error bars. Our analysis therefore shows that the inclusion of realistic error bars, even those from the better dated river fed systems, can cause non-random landslide ages to appear random.

### 3.1.3. Can combination of multiple non-random sets of landslide ages lead to temporal randomness?

We now address our second aim; how easy is it to produce random landslide ages by combining non-random ages from multiple settings? Three different, artificially generated, perfectly periodic non-random distributed (Fig. 3a) landslide datasets were combined and analysed by the  $\chi^2$  statistics. The combined dataset often appeared to be temporally random. The occurrence of an apparently temporally random distribution is the result of the three sources being out of phase with one another. Phase is defined here as the timing of events within a time series. For two perfectly periodic distributions (see Fig. 3a) with recurrence intervals of 1 kyr for both distributions, the distributions would be considered in phase if events in both distributions occurred at the same time (i.e., 1st event at 0.5 ka, 2nd event at 1.5 ka, etc.). They would be considered out of phase if they occurred at different times (i.e., for the first distribution events occurred at 0.5 ka, 1.5 ka, 2.5 ka, etc.; for the second distribution event occurred at 0.3 ka, 1.3 ka, 2.3 ka, etc.). The overlaying of ordered patterns appears to generate

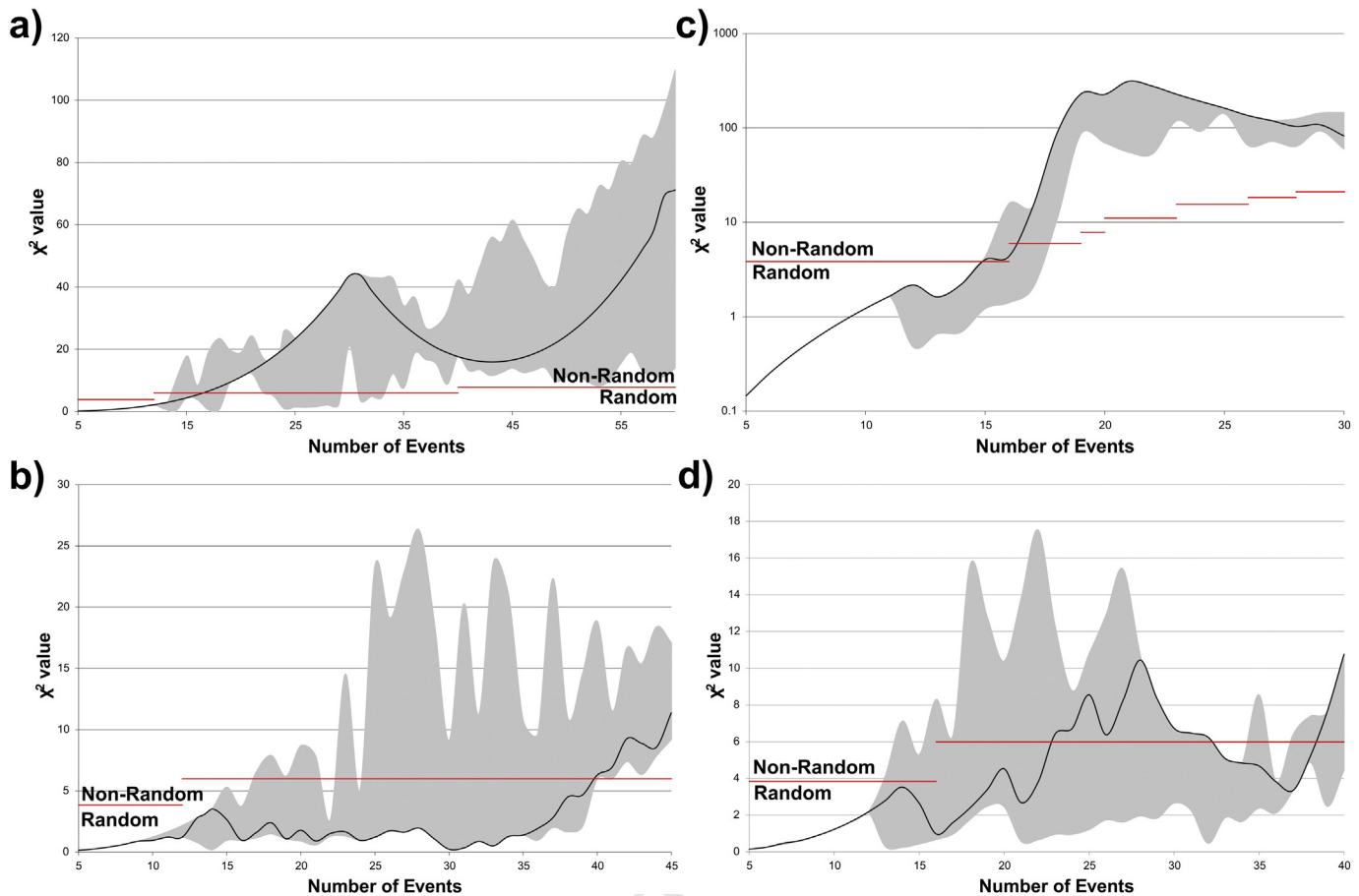


**Fig. 7.** Plot showing the effect of uncertainties up to  $\pm 0.75$  kyr on the different patterns of landslides shown in Fig. 6. The black line represents the  $\chi^2$  statistic value when the ages are known perfectly. The grey areas represent the possible range of  $\chi^2$  statistic values when an uncertainty of  $\pm 0.75$  kyr has been applied. a)  $\chi^2$  statistic values for increasing numbers of landslides in a perfectly periodic pattern. b)  $\chi^2$  statistic values for increasing numbers of landslides in a clustered pattern. c)  $\chi^2$  statistic values for increasing numbers of landslides in a pattern with increasing inter-event times. d)  $\chi^2$  statistic values for increasing numbers of landslides in a patterned patterns. In a–d the red line represents the  $\chi^2$  critical value; one the  $\chi^2$  statistic is above the critical value the pattern of landslides is no longer considered random. (For interpretation of the references to colour in this figure legend, the reader is referred to the web version of this article.)

randomness. Conversely, when perfectly periodic landslide ages were in phase, the distribution of the combined dataset was not perceived to be random.

Age uncertainties were applied, both uniformly across three perfectly periodic landslide datasets and to individual datasets. The latter was intended to replicate the different sized age uncertainties associated with the various margin types seen in [Urlaub et al. \(2013\)](#). Addition of age uncertainty to any or all of the records acted to make the distribution of events appear more temporally random.

This methodology was also applied to the other patterns of landslide ages seen in [Fig. 3](#), in addition to combining datasets with different patterns of landslide ages. The same results were found when three landslide age patterns of the same type were combined. The same was also true when multiple landslide age pattern types were combined. However, assessment of whether one age pattern was in phase with another was problematic.

### 3.2. How many landslide ages are needed to test for a strong dependency on sea level?

To determine the power of the test we performed a series of model iterations. Random introduction of landslides resulted in the distribution of landslide ages appearing temporally random and non-random depending on the order that event were introduced. An example run presented in [Table 3](#). After 23 events are introduced in the example run, the distribution appears to be non-random. However, addition of

another (24th) event then causes the distribution to appear to be random. Only after 28 events does the distribution remain non-random with the additional of further events. We thus recorded the number of events required before the distribution that did not revert to being random following the addition of further events.

Our results showed that the number of landslides needed to indicate a non-random distribution at the 95% confidence interval was highly variable. The mean number required was 38. However, the range of landslides needed was from 10 to 53, with the variability between different iterations being shown by a standard deviation of 8.34; a large figure when compared to the size of the dataset.

These results show that 10 to 53 landslide ages are needed with a mean of 38 ages, when the landslide age is known perfectly to show a strong dependency on sea level. 95% of landslide age distributions were correctly identified as non-random when they had 48 ages. However, the ages from real submarine landslides have are not perfectly dated and have associated error bars ([Urlaub et al., 2013](#)). When these uncertainties are added the number of landslides required to identify a strong sea level dependency will be greater than the number shown here.

## 4. Discussion

We first discuss the implications of the answers to our three aims ([Sections 4.1, 4.2 and 4.3](#)), and then outline the main sources of uncertainty in linking landslide ages and sea level ([Section 4.4](#)). [Section 4.5](#)

**Table 3**

Example of the output from a single iteration using an artificial set of landslide ages whose frequency is linearly proportional to sea level. The number of events column refers to the number of randomly selected ages from the overall distribution which are being analysed by the  $\chi^2$  test. Each row represents the addition of an extra randomly selected age and the output from the  $\chi^2$  test. In this example we can see that when 8 ages are analysed through the  $\chi^2$  test the distribution appears to be non-random. However, addition of further ages causes the distribution to revert to appearing temporally random. Only after 28 ages are added does the distribution appear to be non-random and remain non-random. From this iteration we take 28 ages to be the number of ages required for the  $\chi^2$  test to recognise the distribution is in fact non-random.  $O_j = 0 \dots 4$  is the number of bins observed with  $n$  ages.

Number of events	How the chi-square test views the landslide ages at the 95% confidence interval	Chi-squared value	Critical value	$O_j = 0$	$O_j = 1$	$O_j = 2$	$O_j = 3$	$O_j = 4$	Likelihood-ratio
5	Random	0.136	3.841	26	5				0.036
6	Random	0.237	3.841	25	6				0.452
7	Random	0.38	3.841	24	7				0.497
8	Non-random	13.449	7.815	24	6		1		0.183
9	Non-random	9.658	7.815	23	7		1		5.112
10	Random	7.343	7.815	22	8		1		16.409
11	Random	4.508	7.815	22	7	1	1		2.301
12	Random	3.332	7.815	21	8	1	1		1.961
13	Random	2.565	7.815	21	7	2	1		1.711
14	Random	1.701	7.815	20	8	2	1		1.179
15	Random	1.165	7.815	19	9	2	1		0.867
16	Random	0.905	7.815	18	10	2	1		0.760
17	Random	0.628	7.815	19	9	3	1		2.575
18	Random	1.18	7.815	18	8	4	1		1.184
19	Random	2.416	7.815	18	7	5	1		2.444
20	Random	3.683	7.815	18	7	4	2		2.892
21	Random	4.616	7.815	18	6	5	2		4.229
22	Random	6.156	7.815	18	5	6	2		6.212
23	Non-random	8.123	7.815	18	5	5	3		6.964
24	Random	6.199	7.815	17	6	5	3		5.058
25	Non-random	9.599	7.815	17	6	4	4		6.677
26	Random	7.762	9.488	17	6	4	3	1	6.572
27	Random	7.582	9.488	17	5	5	3	1	6.359
28	Non-random	10.925	9.488	17	5	5	2	2	4.011
29	Non-random	11.697	9.488	17	4	6	2	2	6.447
30	Non-random	12.081	9.488	17	4	5	3	2	6.932
31	Non-random	17.166	9.488	17	4	5	2	3	5.378
32	Non-random	17.325	9.488	17	4	4	3	3	6.254

outlines the most effective strategy for dating landslides, and thus the best way forward.

#### 4.1. Do available dates show that large landslides are random, or are error bars too large?

As might be expected, our results indicated that it was extremely difficult to make non-random patterns of perfectly dated landslides appear temporally random. However, the smallest error bars in the [Urlaub et al. \(2013\)](#) dataset were for 24 river fed systems, with other settings tending to have much larger error bars in landslide ages. We show that such realistic ( $\pm 3$  kyr) error bars resulted in the appearance of random ages, even when landslides were non-random. Thus, the error bars in [Urlaub et al. \(2013\)](#) are too great to tell if these 41 events represent truly random landslides.

##### 4.1.1. The additional impact of bins in making landslides appear temporally random

Additional important errors were introduced into the assessment of whether the events were temporally random by the position of the bins. Bin choice in terms of both width and position is subjective. Therefore it is necessary to vary the position of the bins, up to the bin width in order to assess links between landslides and sea level. Bin width should be chosen depending on the rate of variation in the environmental record (e.g. sea level) with which event frequency is being compared. Bin use, however, remains unavoidable when assessing the statistical distribution of events in a global record (discrete data). Unlike outcrop or single core records, there is no control on the temporal order of events in the global record as deposits do not lie on top of one another. This is compounded by large age uncertainties making the exact temporal order of events unknown. We are therefore unable to use recurrence intervals (continuous data) as the exact relationship between events cannot be specified meaning we

are forced to use statistical tests on the frequency of events within certain specified periods of time, i.e. bins.

#### 4.2. Effects of combining landslide ages from different settings

We demonstrate that three non-random collections of landslide ages could, once combined, appear to be temporally random ([Figs. 5 and 8](#)). More formally, a time-independent, memoryless (Poisson) distribution can result from non-uniform additive influences, as documented by [van Rooij et al. \(2013\)](#). This is likely to be the case for global landslide databases ([Urlaub et al., 2013](#)), and it may be the case for studies based on large-volume turbidites in a single basin centre ([Clare et al., 2014](#)). This conclusion is important as it suggests that a combination of landslide ages from a small number ( $\geq 3$ ) of settings can easily produce a single set of apparently random ages.

##### 4.2.1. Implications for global databases of landslide ages

The global record arguably includes landslides from at least three fundamentally different settings; river-fed systems, ice-stream-fed trough mouth fans and sediment starved margins ([Fig. 5](#)). It is very likely that the relationship between sediment supply and sea level, and hence landslide preconditioning, will vary significantly in these three settings ([Fig. 5](#); [Laberg et al., 2000, 2003](#); [Covault and Graham, 2010](#); [Llopart et al., 2014](#)). Therefore when combined into one record, if the events are out of phase, a temporally random distribution of events is likely. Large age uncertainties will only act to increase the likelihood of such a random distribution in global datasets that consider multiple settings. This suggests that global compilations, or even regional compilations with multiple settings, may not be very useful in determining links between sea level and landslide frequency.

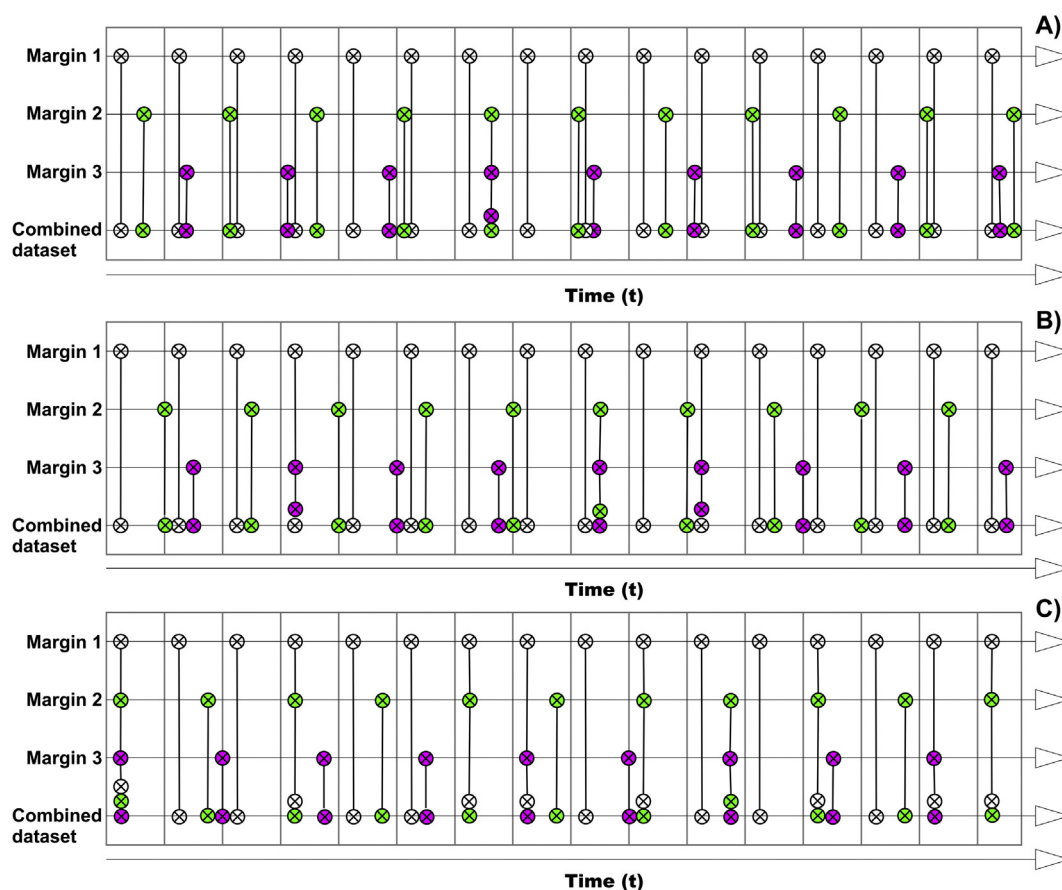


**Fig. 8.** Illustration of how non-random landslides in three settings can be combined to produce random series of landslide ages. Abacus plots showing the combination of landslide ages from three different settings (white, green and pink circles). The lower time series in each panel shows the combined landslide age record. Each setting has landslide ages that are perfectly periodic, but with different recurrence intervals. The setting with the most frequent landslides is shown by the white circles, the setting with the most infrequent events is shown by the pink dots. The grey vertical lines are the edges of 1 kyr bins, which would be used to calculate the histogram of landslide frequencies through time. Parts a, b and c are used to illustrate the importance of differences in phase, as defined by the initial slide event in each series. For example, all three records start in phase in part c, such that they all start with a landslide at the same instant. Part a shows the least in phase landslides, and generates the most strongly temporally random sequence. (For interpretation of the references to colour in this figure legend, the reader is referred to the web version of this article.)

#### 4.2.2. Implications for landslide–turbidite records from a single basin

An alternative approach is to use large turbidites in a single basin, as a proxy for large submarine landslides around the basin margin (Clare et al., 2014; Hunt et al., 2013). However, our study emphasises the importance of understanding the different sources of landslide triggered turbidity currents, if they are out of phase (Rothwell et al., 1998, 2006; Talling et al., 2007; Hunt et al., 2013). Additional effort will also have to be made to clearly identify the difference between landslide and flood triggered turbidites but also to identify where large turbidity currents have been generated by the coalescence of multiple small failures. Inclusion of turbidites in the database that have not been generated by large ( $> 1 \text{ km}^3$ ) events will likely weaken any statistical relationship within a database.

#### 4.3. How many landslides are needed to identify a strong sea level control?

If landslide frequency is linearly proportional to sea level, our study shows that 10 to 53 perfectly dated landslides are needed to statistically identify that direct correlation. It follows that considerably more than 10 to 53 landslides (mean 38) will be needed once age uncertainties are included. However, two other issues are relevant to this discussion.

##### 4.3.1. Controlling factors with more distinctive patterns than sea level

First, further work is needed to determine how many landslides should be dated, if landslide frequency is proportional to rate of sea

level change, and not absolute sea level. More generally, a smaller number of landslides may need to be dated if the controlling factor has a more distinctive pattern through time. Some types of controlling factors may have a more distinctive pattern of variation than near sinusoidal sea level, or occur infrequently. In such cases, a smaller number of landslide ages may be needed to test for statistically significant relationships with landslide frequency. For instance, the Storegga Slide is near synchronous with the last major very abrupt climate change, the 8.2 ka climate event (Haflidason et al., 2005; Dawson et al., 2011). Landslide frequency has also been linked to infrequent periods of very rapid sea level rise (Brothers et al., 2013; Smith et al., 2013). Events of this type are relatively rare and short-lived. A different approach may be needed to determine how many landslides should be dated to see if there is a link to such events.

##### 4.3.2. Stronger proportionality between landslide frequency and sea level

A second issue is that we assume that landslide frequency is directly proportional to sea level, such that the constant proportionality is unity. It is possible that a much stronger association exists, such that the constant proportionality is far greater than unity. In such a situation, a smaller number of landslides may be needed to test for a significant association with sea level.

##### 4.3.3. Local sea level variations and delays in response to sea level

Sea level itself presents challenges for finding a statistical relationship with landslide frequency at a global scale. Local sea level change



can be very different from global eustatic sea level change due to glacio-isostasy and local tectonic influences (Lambeck et al., 1998; Murray-Wallace, 2002). Additional uncertainty arises because of our limited ability to reconstruct accurate local sea level curves. Combined with delayed responses, either to changes in sea level or other identified triggering factors, this reduces the likelihood of linking event to cause. Modelling studies have indicated that continental slopes may have site-specific delayed responses to earthquake triggers (L'Heureux et al., 2013). Delayed and variable response to slow forcing mechanisms such as sea level rise is therefore likely to be even more inconsistent geographically. Submarine landslides from the global catalogue of Urlaub et al. (2013) with relatively well constrained dates are confined to one glacial sea level cycle. Dating of additional events which occurred during other glacial cycles may improve our ability to link events to changes in sea level.

#### 4.4. Implications for studying landslides older than 30 ka

Several reasons may make it problematic to study landslides older than ~30 ka. First, as noted by Urlaub et al. (2013), cores from the modern seafloor may not penetrate deeply enough to reach older events. Second, the error bars in landslide ages tend to increase significantly with time (Fig. 1), especially once landslides become too old to date via radiocarbon (>~43 ka). However, a third reason may also be important.

##### 4.4.1. Non-stationary random triggers whose average recurrence rate varies over time

We have presented a statistical analysis of perfectly non-random landslides and tested the number of landslides that would be required in order to identify non-randomness. However, the testing of these landslide patterns represents an idealised non-random case for two reasons. First, the triggering mechanisms for these events will likely add a random component to these regular patterns. The addition of a degree of randomness, combined with age uncertainties will likely lead to the non-random nature of these events being harder to discern.

Second, landslides may be occurring according to a non-stationary Poisson process. The time period considered within this study is relatively short at geological timescales. The shortness of the time period in question means that the distribution of some random events appears stationary, such that the mean recurrence rate of landslides does not change over time. However, over longer time periods, although remaining inherently random, the mean recurrence rate may change. Such processes are considered to be occurring according to a non-stationary Poisson process, i.e. occurring in clusters (Fig. 3b). Earthquakes represent an example of a non-stationary Poisson process. Over short time periods they have a near-random distribution. Over longer time periods the mean recurrence rate may change as fault systems more or tectonic settings evolve. For submarine landslides, triggering processes are likely to be affected by large-scale environmental change associated with climate change leading to fluctuations in triggering (Geist and Parsons, 2009).

Inherent randomness caused by specific triggers and non-stationarity of Poisson processes mean that the results of this study are somewhat idealised. These results thus represent a best case scenario for recognising non-randomness using the statistical methodology that has been outlined. Detection of a non-stationary Poisson process is not attempted here, and it would be more challenging, and could require many more events than are in Urlaub et al.'s (2013) database. Evaluation of a non-stationary Poisson process for large submarine landslides is difficult, but should be the subject of future work.

##### 4.5. Future strategies for dating submarine landslides – what is the best way forward?

We have shown that realistic error bars in landslide dating, and combination of ages from as few as three different settings, make it difficult

to test for links between sea level and landslide frequency. The most complete global compilation of 41 large landslide ages in the last 30 ka appears temporally random (Urlaub et al., 2013), but could plausibly result from non-random processes such as sea level. We currently have too few well-dated landslides to test for a linear dependence between landslide frequency and sea level, even using better constrained sub-sets of those landslide ages from river fed systems (Urlaub et al., 2013). Although we would be able to test for a stronger (i.e. non-linear) dependence on sea level, or indeed links to events with more distinctive time series, such as abrupt climate warming or sea level rise events. However, these negative conclusions raise the issue; what is the most constructive way forward?

##### 4.5.1. Testing scientific hypotheses – are negative results useful?

We first note that it is useful to know the answer to scientific questions, even when they are negative answers. This helps us to narrow down avenues of future research, and avoid misleading conclusions, such as that currently available landslide ages show a significant correlation with sea level. Indeed, a broad comparison might be made to medical trials, in which there is a detrimental bias towards publications of positive tests (Goldacre, 2010).

##### 4.5.2. Importance of using quantitative and robust statistical methods

Previous workers have proposed a number of different relationships between sea level and landslide frequency, based on qualitative analyses. They include a relationship between landslides and low sea level (Paull et al., 1996), rising or low sea level (Lee, 2009), or indeed no relationship with sea level (Urlaub et al., 2013). This study illustrates the importance of quantitative statistical techniques to understand what is significant in such datasets.

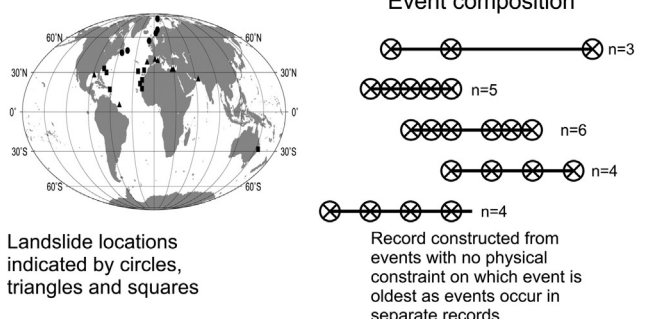
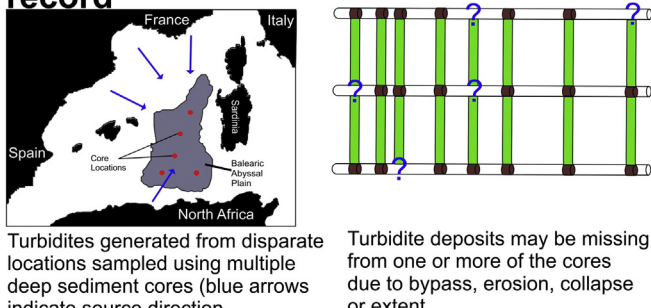
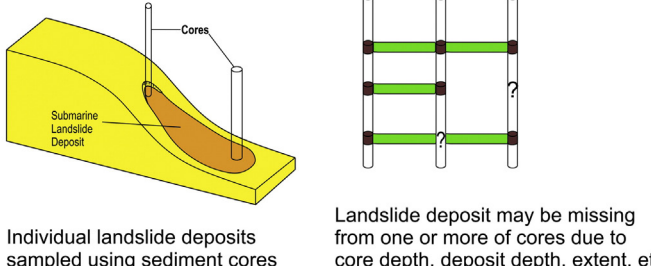
More sophisticated statistical methodologies can be used. For example treating submarine landslide hazards in a similar evidence-based manner to large magnitude volcanic and earthquake hazards (Aspinall et al., 2003; Baxter et al., 2008; Daub et al., 2012). Evidence-based refers to a methodology where the examination of evidence from specific studies and the systematic collection of this evidence are highly weighted in decision making; intuition and unsystematic experience are de-emphasised (Sackett et al., 1996). Evidence based hazard analysis, first used in medicine (Aspinall et al., 2003) and subsequently used on Montserrat from 1997 (Baxter et al., 2008), incorporates all available theoretical and observational information and applies probabilistic procedures using Bayesian statistics. This allows decision making that is open to revision with partial or imperfect information as the degree of evidence uncertainty is weighted accordingly (Baxter et al., 2008). Hazard assessment should therefore attempt to incorporate well dated landslides, including those whose ages are near abrupt climatic events whilst also including extreme value theory statistics (Sornette, 2009; Dawson et al., 2011; Bondevik et al., 2012).

##### 4.5.3. Should there be a wider spread of dated landslides to avoid spatially biased compilations?

The current global compilation of landslides ages is spatially biased (Urlaub et al., 2013). Large submarine landslides have predominantly been catalogued in certain areas, such as the North Atlantic, Iberian Margin, and Mediterranean (Fig. 9) (Urlaub et al., 2013). International efforts could therefore attempt to broaden the area where events are dated, and avoid such strong geographical biases. However, this might not be the most productive strategy as it will result in the combination of landslide ages from an even wider range of settings. As we show here, a greater number of settings may be very likely to generate apparently random age sequences from non-random triggers (Figs. 5 and 9).

##### 4.5.4. Concentration of dating efforts at a small number of similar settings with long records

Our study suggests that efforts may need to be concentrated, such that statistically significant numbers of well-dated landslides are

<b>Global Record</b>  Record length: 30 ka Number of events: 41 Return period: ?	<b>Global record</b>    Landslide locations indicated by circles, triangles and squares  Event composition n=3 n=5 n=6 n=4 Record constructed from events with no physical constraint on which event is oldest as events occur in separate records	<b>Issues with record</b>  Geographical bias Temporally limited Limited by sample size
<b>Regional Record</b>  Record length: $\geq 250$ ka Number of events: $>100$ Return period: $\geq 1000$ a	<b>Sampling regional record</b>    Turbidites generated from disparate locations sampled using multiple deep sediment cores (blue arrows indicate source direction)  Regional core correlation Turbidite deposits may be missing from one or more of the cores due to bypass, erosion, collapse or extent	<b>Issues with record</b>  Limited to size $>0.1 \text{ km}^3$ i.e. flows of sufficient size to reach the basin Overprinting of signal i.e. multiple sources with possibly varying signals
<b>Local Record</b>  Record length: Core dependent Number of events: $<10$ Return period: location dependent	<b>Sampling method of local data</b>    Individual landslide deposits sampled using sediment cores  Core correlations Landslide deposit may be missing from one or more of cores due to core depth, deposit depth, extent, etc	<b>Issues with record</b>  Typically limited to 1-2 slides Age constraints/dating errors Limited by core depth

**Fig. 9.** A simplified schematic of the existing issues associated at different spatial scales linking submarine landslide frequency to changing environmental factors. Problems associated with each of the different records have emerged as introducing significant error during different parts of this study.

obtained from individual types of setting. To achieve this, controlling variables need to be isolated; something the use of disparate records may prevent (McAdoo and Watts, 2004; Brothers et al., 2013). Perhaps the simplest means of advancing knowledge is to focus specifically on river fed systems (Covault and Graham, 2010). River fed systems have both the greatest number of catalogued events, as well as the smallest age uncertainties (Urlaub et al., 2013). They are also the margin type where glacial cycles have been suggested to play a particularly important role, via sediment supply (Covault and Graham, 2010). Identification of additional events at these margins therefore provides the greatest likelihood of asserting, with some degree of confidence, the effects of sea level on landslide frequency (Geist et al., 2013). This could be achieved through either IODP sites or long basin core records where the input sources to the basin are well constrained. Focusing on one of these record types and isolating local environmental factors such as local sea level change would allow for a more useful comparison of landslide frequency and sea level change. However, care will still be needed to be taken to distinguish the effects of glacio-eustatic sea level on slope stability, and factors that co-vary with glacial cycles, such as the rate of sediment supply from rivers (Covault and Graham, 2010).

#### 4.5.5. Should we date fewer landslides, but with greater precision?

This question is important because finite resources can be directed towards obtaining a greater number of (lower precision) landslide ages, or a small number of very well-dated examples. This study does not provide a full statistical analysis of such a logistical trade-off. However, it is important that marginally increasing the number of poorly dated landslides in global compilations, with uncertainties that are well in excess of  $\pm 3$  kyr, may not be a constructive way forward. For instance, our work suggest that around 40 well-dated ( $\pm 0.75$  kyr) landslides from a single setting would be necessary to allow robust statistical analysis of links between sea level and landslide frequency. Long records from specific locations with multiple events are therefore the most appropriate for isolating triggering mechanisms.

## 5. Conclusions

Previous work found that the most complete compilation of 41 ( $>1 \text{ km}^3$ ) submarine landslide ages in the last 30 ka suggests that these hazardous events are temporally random (Urlaub et al., 2013). However, it was unclear whether the landslides were temporally

random, or whether the considerable uncertainties on most landslide ages made it impossible to tell. The primary conclusion of this study is that there are currently too few, sufficiently well-dated large landslides, to know whether these large submarine landslides are temporally random. The addition of realistic error bars to the ages of landslides that are non-random, can produce ages that appear temporally random.

Second, we show that it is likely that combination of landslide ages from different settings, each with different preconditioning and triggering factors that are offset in time, can easily produce a combined dataset that appears random in time. We show that just three distinct settings may be combined to produce apparently temporally random dates. This is important because most global databases of landslide ages probably include at least three distinct types of setting.

Third, we constrain the number of landslides, needed to test whether there is significant correlation between landslide frequency and global sea level. This was done simulating landslide ages that are correlated perfectly with sea level. The number of such landslide ages needed to test for a significant correlation with sea level ranged from 10 to 53, with a mean of 38, even when landslide ages were known perfectly.

Finally, we provide some suggestions for the best future strategy for assessing the submarine landslide hazard. We suggest focussing on specific environment settings, and on a smaller number of well-dated landslides (~40) to test for links with sea level.

The results of this study indicate the issues inherent with using the global record of submarine landslide occurrence in its current form. Our results indicate that both realistic age uncertainties and combination of data from multiple settings may make it hard to test for links between sea level and landslide frequency. However, it may be easier to test links between landslide frequency and more episodic and shorter duration events, such as the 8.2 kyr climate event or meltwater pulse 1, which have more distinctive time-series than sea level. Finally, the best means to understand links between sea level and landslide frequency may come from local studies with more numerous recurrence intervals (e.g. Clare et al., 2014, 2015), perhaps in conjunction with detailed records of localised environmental change.

## Q9 6. Uncited reference

Carter et al., 2012

## Acknowledgements

We would like to thank three anonymous reviewers. Their comments and suggestions greatly improved the manuscript. E. Pope was supported by the NERC Arctic Research Programme under project on whether climate change increases the landslide-tsunami risk to the UK (NE/K00008X/1). This research was completed as part of the EU FP7-funded ASTARTE (Assessment, Strategy and Risk Reduction for Tsunamis in Europe) Project.

## References

- Aspinall, W.P., Woo, G., Voight, B., Baxter, P.J., 2003. Evidence-based volcanology: application to eruption crises. *J. Volcanol. Geotherm. Res.* 128, 273–285.
- Baxter, P.J., Aspinall, W.P., Neri, A., Zuccaro, G., Spence, R.J.S., Cioni, R., Woo, G., 2008. Emergency planning and mitigation at Vesuvius: a new evidence-based approach. *J. Volcanol. Geotherm. Res.* 178, 454–473.
- Beget, J.E., Addison, J.A., 2007. Methane gas release from the Storegga submarine landslide linked to early-Holocene climate change: a speculative hypothesis. *The Holocene* 17, 291–295.
- Boe, R., Prosch-Danielsen, L., Lepland, A., Harbitz, C.B., Gauer, P., Lovholt, F., Hogestol, M., 2007. An early Holocene submarine slide in Boknafjorden and the effect of a slide-triggered tsunami on Stone Age settlements at Rennesøy, SW Norway. *Mar. Geol.* 243, 157–168.
- Bondevik, S., Stormo, S.K., Skjerdal, G., 2012. Green mosses date the Storegga tsunami to the chilliest decades of the 8.2 ka cold event. *Quat. Sci. Rev.* 45, 1–6.
- Bourget, J., Zaragosi, S., Ellouz-Zimmermann, N., Mouchot, N., Garlan, T., Schneider, J.L., Lanfume, V., Lallemand, S., 2011. Turbidite system architecture and sedimentary processes along topographically complex slopes: the Makran convergent margin. *Sedimentology* 58, 376–406.

- Brothers, D.S., Luttrell, K.M., Chaytor, J.D., 2013. Sea-level-induced seismicity and submarine landslide occurrence. *Geology* 41, 979–982.
- Bruschi, R., Bughi, S., Spinazzè, M., Torselletti, E., Vitali, L., 2006. Impact of debris flows and turbidly currents on seafloor structures. *Norsk Geologisk Tidsskrift* 86, 317.
- Carter, L., Burnett, D., Drew, S., Hagadorn, L., Marle, G., Bertlett-McNeil, D., Irvine, N., 2009. Submarine Cables and the Oceans – Connecting the World: UNEP-WCMC Biodiversity Series 311CPC/UNEP/UNEP-WCMC, p. 64.
- Carter, L., Milliman, J.D., Talling, P.J., Gavey, R., Wynn, R.B., 2012. Near-synchronous and delayed initiation of long run-out submarine sediment flows from a record-breaking river flood, offshore Taiwan. *Geophys. Res. Lett.* 39.
- Clare, M.A., Talling, P.J., Challenor, P., Malgesini, G., Hunt, J.E., 2014. Distal turbidites reveal a common distribution for large (>0.1 km<sup>3</sup>) submarine landslide recurrence. *Geology* 42, 263–266.
- Clare, M.A., Talling, P.J., Hunt, J.E., 2015. Implications of reduced turbidity current and landslide activity for the Initial Eocene Thermal Maximum—evidence from two distal, deep-water sites. *Earth Planet. Sci. Lett.* 420, 102–115.
- Clarke, S., Hubble, T., Airey, D., Yu, P., Boyd, R., Keene, J., Exon, N., Gardner, J., 2012. Submarine Landslides on the Upper Southeast Australian Passive Continental Margin—preliminary Findings, Submarine Mass Movements and Their Consequences. Springer, pp. 55–66.
- Covault, J.A., Graham, S.A., 2010. Submarine fans at all sea-level stands: tectono-morphologic and climatic controls on terrigenous sediment delivery to the deep sea. *Geology* 38, 939–942.
- Daub, E.G., Ben-Naim, E., Guyer, R.A., Johnson, P.A., 2012. Are megaquakes clustered? *Geophys. Res. Lett.* 39.
- Dawson, A., Bondevik, S., Teller, J., 2011. Relative timing of the Storegga submarine slide, methane release, and climate change during the 8.2 ka cold event. *The Holocene* 21, 1167–1171.
- Dowdeswell, J.A., Kenyon, N.H., Elverhøi, A., Laberg, J.S., Hollender, F.J., Mienert, J., Siegert, M.J., 1996. Large-scale sedimentation on the glacier-influenced polar North Atlantic Margins: long-range side-scan sonar evidence. *Geophys. Res. Lett.* 23, 3535–3538.
- Garziglia, S., Migeon, S., Ducassou, E., Loncke, L., Mascle, J., 2008. Mass-transport deposits on the Rosetta province (NW Nile deep-sea turbidite system, Egyptian margin): characteristics, distribution, and potential causal processes. *Mar. Geol.* 250, 180–198.
- Geist, E.L., Parsons, T., 2009. Assessment of source probabilities for potential tsunamis affecting the US Atlantic coast. *Mar. Geol.* 264, 98–108.
- Geist, E.L., Chaytor, J.D., Parsons, T., ten Brink, U., 2013. Estimation of submarine mass failure probability from a sequence of deposits with age dates. *Geosphere* 9, 287–298.
- Goldacre, B., 2010. Bad Science: Quacks, Hacks, and Big Pharma Flacks. McClelland & Stewart.
- Goldfinger, C., 2011. Submarine paleoseismology based on turbidite records. *Ann. Rev. Mar. Sci.* 3 (3), 35–66.
- Gracia, E., Vizcaino, A., Escutia, C., Asioli, A., Rodes, A., Pallas, R., Garcia-Orellana, J., Lebreiro, S.M., Goldfinger, C., 2010. Holocene earthquake record offshore Portugal (SW Iberia): testing turbidite paleoseismology in a slow-convergence margin. *Quat. Sci. Rev.* 29, 1156–1172.
- Hafliðason, H., Lien, R., Sejrup, H.P., Forsberg, C.F., Bryn, P., 2005. The dating and morphometry of the Storegga Slide. *Mar. Pet. Geol.* 22, 123–136.
- Hampton, M.A., Lee, H.J., Locat, J., 1996. Submarine landslides. *Rev. Geophys.* 34, 33–59.
- Hornbach, M.J., Lavier, L.L., Ruppel, C.D., 2007. Triggering mechanism and tsunamogenic potential of the Cape Fear Slide complex, US Atlantic margin. *Geochim. Geophys. Geosyst.* 8.
- Hsu, S.K., Kuo, J., Lo, C.L., Tsai, C.H., Doo, W.B., Ku, C.Y., Sibuet, J.C., 2008. Turbidity currents, submarine landslides and the 2006 Pingtung earthquake off SW Taiwan. *Terr. Atmos. Ocean. Sci.* 19, 767–772.
- Hühnerbach, V., Masson, D.G., 2004. Landslides in the North Atlantic and its adjacent seas: an analysis of their morphology, setting and behaviour. *Mar. Geol.* 213, 343–362.
- Hunt, J.E., Wynn, R.B., Talling, P.J., Masson, D.G., 2013. Frequency and timing of landslide-triggered turbidity currents within the Agadir Basin, offshore NW Africa: are there associations with climate change, sea level change and slope sedimentation rates? *Mar. Geol.* 346, 274–291.
- Kendall, M., Stuart, A., Ord, J., Arnold, S., 1999. Vol. 2A: Classical Inference and the Linear Model. Arnold [etc.], London [etc.].
- Kennett, J.P., Cannariato, K.G., Hendy, I.L., Behl, R.J., 2000. Carbon isotopic evidence for methane hydrate instability during quaternary interstadials. *Science* 288, 128–133.
- Korup, O., 2012. Earth's portfolio of extreme sediment transport events. *Earth Sci. Rev.* 112, 115–125.
- Laberg, J.S., Vorren, T.O., Dowdeswell, J.A., Kenyon, N.H., Taylor, J., 2000. The Andoya Slide and the Andoya Canyon, north-eastern Norwegian-Greenland Sea. *Mar. Geol.* 162, 259–275.
- Laberg, J.S., Vorren, T.O., Mienert, J., Hafliðason, H., Bryn, P., Lien, R., 2003. Preconditions leading to the Holocene Trænadjupet Slide offshore Norway. In: Locat, J., Mienert, J., Boisvert, L. (Eds.), *Submarine Mass Movements and Their Consequences*. Springer, Netherlands, pp. 247–254.
- Lambeck, K., Smither, C., Johnston, P., 1998. Sea-level change, glacial rebound and mantle viscosity for northern Europe. *Geophys. J. Int.* 134, 102–144.
- Lastras, G., Canals, M., Urgeles, R., De Batist, M., Calafat, A., Casamor, J., 2004. Characterisation of the recent BIG95 debris flow deposit on the Ebro margin, Western Mediterranean Sea, after a variety of seismic reflection data. *Mar. Geol.* 213, 235–255.
- Lebreiro, S.M., Voelker, A.H.L., Vizcaino, A., Abrantes, F.G., Alt-Epping, U., Jung, S., Thouveny, N., Gracia, E., 2009. Sediment instability on the Portuguese continental margin under abrupt glacial climate changes (last 60 kyr). *Quat. Sci. Rev.* 28, 3211–3223.
- Lee, H.J., 2009. Timing of occurrence of large submarine landslides on the Atlantic Ocean margin. *Mar. Geol.* 264, 53–64.



- Leynaud, D., Mienert, J., Vanneste, M., 2009. Submarine mass movements on glaciated and non-glaciated European continental margins: a review of triggering mechanisms and preconditions to failure. *Mar. Pet. Geol.* 26, 618–632.
- L'Heureux, J.S., Vanneste, M., Rise, L., Brendryen, J., Forsberg, C.F., Nadim, F., Longva, O., Chand, S., Kvalstad, T.J., Hafliðason, H., 2013. Stability, mobility and failure mechanism for landslides at the upper continental slope off Vesterålen, Norway. *Mar. Geol.* 346, 192–207.
- Llopert, J., Urgeles, R., Camerlenghi, A., Lucchi, R.G., Mol, B., Rebescio, M., Pedrosa, M.T., 2014. Slope instability of glaciated continental margins: constraints from permeability–compressibility tests and hydrogeological modeling off Storfjorden, NW Barents Sea. In: Krastel, S., Behrmann, J.-H., Völker, D., Stipp, M., Berndt, C., Urgeles, R., Chaytor, J., Huhn, K., Strasser, M., Harbitz, C.B. (Eds.), *Submarine Mass Movements and Their Consequences*. Springer International Publishing, pp. 95–104.
- Maslin, M., Mikkelsen, N., Vilela, C., Haq, B., 1998. Sea-level- and gas-hydrate-controlled catastrophic sediment failures of the Amazon Fan. *Geology* 26, 1107–1110.
- Maslin, M., Owen, M., Day, S., Long, D., 2004. Linking continental-slope failures and climate change: testing the clathrate gun hypothesis. *Geology* 32, 53–56.
- Maslin, M., Vilela, C., Mikkelsen, N., Grootes, P., 2005. Causes of catastrophic sediment failures of the Amazon Fan. *Quat. Sci. Rev.* 24, 2180–2193.
- Masson, D.G., Harbitz, C.B., Wynn, R.B., Pedersen, G., Lovholt, F., 2006. Submarine landslides: processes, triggers and hazard prediction. *Philos. Trans. R. Soc. A Math. Phys. Eng. Sci.* 364, 2009–2039.
- Masson, D.G., Arzola, R.G., Wynn, R.B., Hunt, J.E., Weaver, P.P.E., 2011. Seismic triggering of landslides and turbidity currents offshore Portugal. *Geochim. Geophys. Geosyst.* 12.
- McAdoo, B.G., Watts, P., 2004. Tsunami hazard from submarine landslides on the Oregon continental slope. *Mar. Geol.* 203, 235–245.
- Murray-Wallace, C.V., 2002. Pleistocene coastal stratigraphy, sea-level highstands and neotectonism of the southern Australian passive continental margin—a review. *J. Quat. Sci.* 17, 469–489.
- Owen, M., Day, S., Maslin, M., 2007. Late Pleistocene submarine mass movements: occurrence and causes. *Quat. Sci. Rev.* 26, 958–978.
- Parker, E.J., Traverso, C.M., Giudice, T.D., Evans, T., Moore, R., 2009. Geohazard Risk Assessment — Vulnerability of Subsea Structures to Geohazards — Risk Implications.
- Paull, C.K., Buelow, W.J., Ussler, W., Borowski, W.S., 1996. Increased continental-margin slumping frequency during sea-level lowstands above gas hydrate-bearing sediments. *Geology* 24, 143–146.
- Paull, C.K., Ussler, W., Holbrook, W.S., 2007. Assessing methane release from the colossal Storegga submarine landslide. *Geophys. Res. Lett.* 34.
- Pecher, I.A., Henrys, S.A., Ellis, S., Chiswell, S.M., Kukowski, N., 2005. Erosion of the seafloor at the top of the gas hydrate stability zone on the Hikurangi Margin, New Zealand. *Geophys. Res. Lett.* 32.
- Piper, D.J.W., Cochonat, P., Morrison, M.L., 1999. The sequence of events around the epicentre of the 1929 Grand Banks earthquake: initiation of debris flows and turbidity current inferred from sidescan sonar. *Sedimentology* 46, 79–97.
- Ramsey, C.B., 1998. Probability and dating. *Radiocarbon* 40, 461–474.
- Reeder, M.S., Rothwell, R.G., Stow, D.A.V., 2000. Influence of sea level and basin physiography on emplacement of the late Pleistocene Herodotus Basin Megaturbidite, SE Mediterranean Sea. *Mar. Pet. Geol.* 17, 199–218.
- Reeder, M.S., Stow, D.A.V., Rothwell, R.G., 2002. Late Quaternary turbidite input into the east Mediterranean basin: new radiocarbon constraints on climate and sea-level control. *Geol. Soc. Lond. Spec. Publ.* 191, 267–278.
- Rothwell, R.G., Thomson, J., Kähler, G., 1998. Low-sea-level emplacement of a very large Late Pleistocene 'megaturbidite' in the western Mediterranean Sea. *Nature* 392, 377–380.
- Rothwell, R.G., Hoogakker, B., Thomson, J., Croudace, I.W., Frenz, M., 2006. Turbidite emplacement on the southern Balearic Abyssal Plain (western Mediterranean Sea) during Marine Isotope Stages 1–3: an application of ITRAX XRF scanning of sediment cores to lithostratigraphic analysis. *Geol. Soc. Lond. Spec. Publ.* 267, 79–98.
- Ruffman, A., 2001. Potential for large-scale submarine slope failure and tsunami generation along the US mid-Atlantic coast: Comment. *Geology* 29, 967–967.
- Sackett, D.L., Rosenberg, W., Gray, J.A., Haynes, R.B., Richardson, W.S., 1996. Evidence based medicine: what it is and what it isn't. *BMJ* 312, 71–72.
- Smith, D.E., Harrison, S., Jordan, J.T., 2013. Sea level rise and submarine mass failures on open continental margins. *Quat. Sci. Rev.* 82, 93–103.
- Sornette, D., 2009. Dragon-kings, black swans and the prediction of crises. *arXiv, preprint arXiv:0907.4290*.
- Stigall, J., Dugan, B., 2010. Overpressure and earthquake initiated slope failure in the Ursa region, northern Gulf of Mexico. *J. Geophys. Res. Solid Earth* 115.
- Sumner, E.J., Siti, M.I., McNeill, L.C., Talling, P.J., Henstock, T.J., Wynn, R.B., Djajadihardja, Y.S., Permana, H., 2013. Can turbidites be used to reconstruct a paleoearthquake record for the central Sumatran margin? *Geology* 41, 763–766.
- Swan, A.R.H., Sandilands, M., 1995. *Introduction to Geological Data Analysis*. Blackwell Science, Oxford; Cambridge, Mass, USA.
- Talling, P.J., Wynn, R.B., Masson, D.G., Frenz, M., Cronin, B.T., Schiebel, R., Akhmetzhanov, A.M., Dallmeier-Tiessen, S., Benetti, S., Weaver, P.P.E., Georgiopoulou, A., Zuhlsdorff, C., Amy, L.A., 2007. Onset of submarine debris flow deposition far from original giant landslide. *Nature* 450, 541–544.
- Talling, P.J., Masson, D.G., Sumner, E.J., Malgesini, G., 2012. Subaqueous sediment density flows: depositional processes and deposit types. *Sedimentology* 59, 1937–2003.
- Talling, P.J., Clare, M.A., Urlaub, M., Pope, E., Hunt, J.E., Watt, S.F.L., 2014. Large submarine landslides on continental slopes. *Oceanography* 27, 32.
- Tappin, D.R., Watts, P., McMurtry, G.M., Lafoy, Y., Matsumoto, T., 2001. The Sissano, Papua New Guinea tsunami of July 1998 — offshore evidence on the source mechanism. *Mar. Geol.* 175, 1–23.
- Urlaub, M., Zervos, A., Talling, P.J., Masson, D.G., Clayton, C.I., 2012. How do ~2° slopes fail in areas of slow sedimentation? A sensitivity study on the influence of accumulation rate and permeability on submarine slope stability. In: Yamada, Y., Kawamura, K., Ikehara, K., Ogawa, Y., Urgeles, R., Mosher, D., Chaytor, J., Strasser, M. (Eds.), *Submarine Mass Movements and Their Consequences*. Springer, Netherlands, pp. 277–287.
- Urlaub, M., Talling, P.J., Masson, D.G., 2013. Timing and frequency of large submarine landslides: implications for understanding triggers and future geohazard. *Quat. Sci. Rev.* 72, 63–82.
- van Rooij, M.J.W., Nash, B.A., Rajaraman, S., Holden, J.G., 2013. A fractal approach to dynamic inference and distribution analysis. *Front. Physiol.* 4.
- Vanneste, M., Mienert, J., Büinz, S., 2006. The Hinlopen Slide: a giant, submarine slope failure on the northern Svalbard margin, Arctic Ocean. *Earth Planet. Sci. Lett.* 245, 373–388.
- Völker, D., Scholz, F., Geersen, J., 2011. Analysis of submarine landsliding in the rupture area of the 27 February 2010 Maule earthquake, Central Chile. *Mar. Geol.* 288, 79–89.
- Waelbroeck, C., Labeyrie, L., Michel, E., Duplessy, J.C., McManus, J.F., Lambeck, K., Balbon, E., Labracherie, M., 2002. Sea-level and deep water temperature changes derived from benthic foraminifera isotopic records. *Quat. Sci. Rev.* 21, 295–305.
- Weaver, P.P.E., Kuijpers, A., 1983. Climatic control of turbidite deposition on the Madeira Abyssal Plain. *Nature* 306, 360–363.